Promoting the Allowable Stress Method for the Design of Glass Members and Frameless Structures

Saddam Hussain
Department of Civil Engineering and Architecture, Kyushu Institute of Technology

Chen, Pei Shan
Department of Civil Engineering and Architecture, Kyushu Institute of Technology

Chiara Bedon
Department of Engineering and Architecture, University of Trieste

Hassan Javed
Department of Civil Engineering, Lahore Leads University

https://doi.org/10.5109/7323373

出版情報：Proceedings of International Exchange and Innovation Conference on Engineering & Sciences (IEICES). 10, pp.943-949, 2024-10-17. International Exchange and Innovation Conference on Engineering & Sciences
バージョン：

Promoting the Allowable Stress Method for the Design of Glass Members and Frameless Structures

Saddam Hussain[1*], Pei Shan Chen[1], Chiara Bedon[2*], Hassan Javed[3]

[1] Department of Civil Engineering and Architecture, Kyushu Institute of Technology, Kitakyushu, Japan
[2] Department of Engineering and Architecture, University of Trieste, Trieste, Italy
[3] Department of Civil Engineering, Lahore Leads University, Thokar Niaz Baig, Pakistan
Corresponding author email: saddam.hussain372@mail.kyutech.jp, chiara.bedon@dia.units.it

Abstract: *This study promotes the construction of transparent spatial structures with a minimum use of metal frameworks, by employing glass panels as primary members. The Allowable Stress Method, which is used to verify building components made of different materials, but is not available for glass members, is also proposed. In this regard, a sound theoretical investigation on tempered glass members under in-plane bending and lateral-torsional buckling (LTB) is summarized. Original experiments are used in support of the load-carrying capacity analysis of glass specimens. Their LTB failure is also addressed, as a function of slenderness ratio, to derive the allowable stress function. As shown, the presented findings result in robust equations for determining the allowable stress of tempered panels in bending, and in a general approach that can be extended to various loading conditions. The proposed methodology is finally applied to the exemplificative structural design of a three-dimensional frameless roof.*

Keywords: Frameless Glass Structures; Allowable Bending Stress; Lateral-Torsional Buckling (LTB); Structural Design; Long-term and short-term loads

1. INTRODUCTION

1.1 Conventional or Frameless Glass Structures

In last decades, glass changed its role of typical secondary building material into a key solution for architectural innovation and novel structural concepts. Its role rapidly expanded beyond mere transparency needs, contributing to sophisticated aesthetics in architectural arrangements and use for load-bearing components, with other traditional materials. Fig. 1(a) depicts typical conventional metal framed glass structures, which worldwide demonstrate the impact of glass in contemporary architecture, ranging from famous all-glass facades to spectacular bridge attractions, and its combined powerful use with metal structures [1-13].

(a) Conventional glass structures supported by metal frames.

(b) Frameless glass structures.

Fig. 1. Examples of different glass structures [1, 2].

To meet the requirement of high transparency, frameless glass structures are also increasingly promoted. As shown in Fig. 1(b), recent and well-known examples can be found in existing assemblies like the Apple Store and the Glass Canopy in Tokyo (©2023 Rafael Vinoly Architects).

To address the challenge of high transparency and aesthetics for these innovative spatial structures, see Fig. 2, researchers from Chen's Laboratory are drawing inspiration and guidance from ancient structural principles [3].

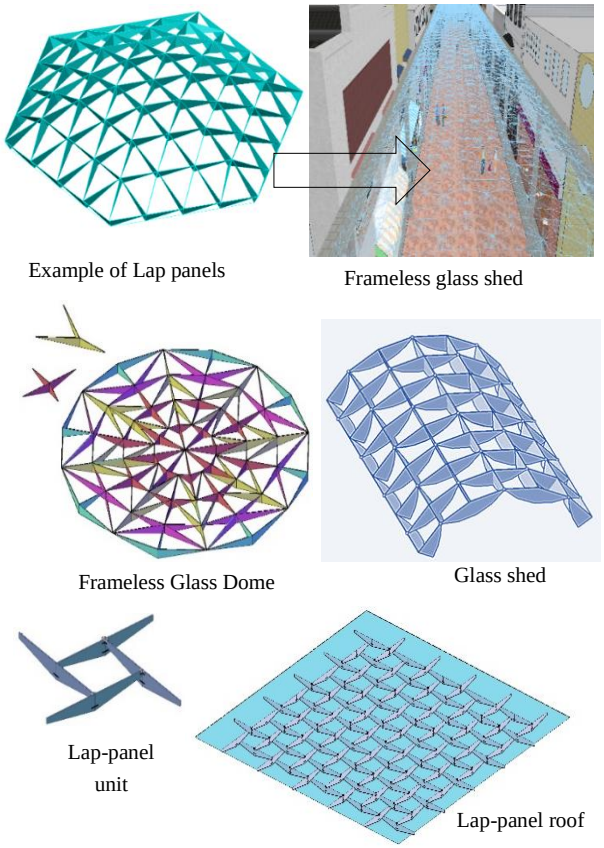

Fig. 2. Examples of spatial frameless glass structures.

The Lap-panel system inspired by the ancient wooden bridges like the Hongqiao, for example, can support innovative solutions for modern structural systems (Fig. 2). The Reciprocal Panel system in Fig. 2, which is also derived from reciprocal frame concepts of Eastern and Western cultures, provides an alternative sound framework for assembling frameless glass structures that combine heritage-inspired design with modern engineering and architectural principles [2].

1.2 Glass Types and Production

As known, glass production methods significantly impact on its mechanical and thermo-physical properties, and have major consequences on structural and architectural design considerations. Float glass, which is commonly used for ordinary windows, doors, partition walls, is made by pouring molten glass onto a tin bath, and ensuring uniform thickness and surface quality to the obtained flat panels. Tempered glass undergoes indeed a typical heat treatment process, which involves compression on the surface and tension in the core of the resisting section (Fig. 3). This distribution of internal stresses largely enhances its strength, compared to non-prestressed glass, with about 4 times enhanced performance [4-7]. For frameless glass structures, as in the present study, tempered glass can thus serve as principal construction material.

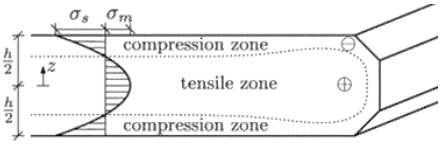

Fig. 3. Typical stress distribution in tempered glass.

1.3 Design of Frameless Glass Structures

In practice, structural verifications are essential to ensure appropriate safety and stability to building components and systems against design loads, and allowable stress calculations often represent a fundamental procedure for many traditional constructional materials. As shown in Fig. 4, the present study promotes a process of structural design for glass frameless structures which is based on the equivalent beam concept, and includes allowable stress calculations [7-12].

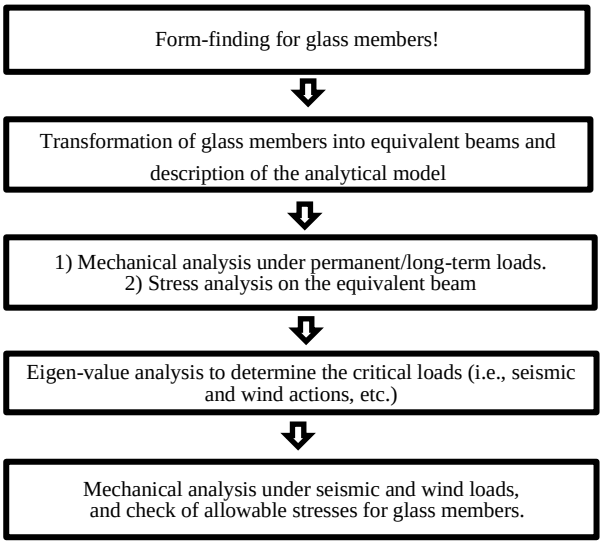

Fig. 4. Structural design processes for frameless glass structures.

1.4 Research Purpose and Methods

The present investigation is based on the consideration that in common structural design standards and technical documents there are several types and definitions of "allowable stress" for load-bearing members, including those for bending, compression, tension, etc. This research focuses specifically on allowable bending stress considerations, for tempered glass panels under in-plane loading, as there is no literature research in this direction. The primary goal is thus to determine a robust and general methodology to calculate the allowable stress for pure bending in glass members. In addition, the study focuses on understanding the load-carrying mechanisms and failure mode under lateral-torsional buckling (LTB), which is a critical condition associated to pure bending moments.

As shown, the proposed methodology takes a major advantage from properly designed experiments for tempered glass beam-like panels that are subjected to in-plane loading conditions, while allowing their rotation and translation at the ends. Through the experimental testing of specimens (also with various geometrical features), key mechanical properties that are relevant to structural analysis, such as bending and LTB performances, are evaluated. Subsequently, the research summarizes the adopted approach for calculating the allowable bending stress for design, based on statistical analysis of experimental results. The final objective is to establish a robust equation for evaluating the allowable bending stress in frameless glass members, thereby enhancing their safety and practical application, and possibly extend the same procedure to various loading configurations.

Glass inherent brittleness can in fact lead to abrupt and premature collapse. The herein reported investigation, in this regard, aims to contribute to establish standardized protocols by devising specialized approaches for determining appropriate stress design limits, through comprehensive testing, analysis and modelling. Ultimately, an exemplificative trial structural design is in fact proposed, for a three-dimensional frameless roof, showing the potential of the developed methodology.

2. BASIC PRINCIPLES OF LTB

For slender load-bearing members, such as glass beam-like components, LTB represents a critical failure configuration that should be properly verified. Fig. 5, in this regard, illustrates the pure bending behaviour of a rectangular glass beam (span l, cross-section $h \times t$) under in-plane loading, which could critically fail for LTB.

The undeformed configuration of the beam is defined by the coordinate system x, y, z; following LTB, the deformed axes change to x', y', z'.

The torsional angle ϕ, the vertical displacement v and the lateral displacement u are the key performance indicators. The critical load/moment can be obtained from the classical differential equations of equilibrium of the deformed beam. The relation between the moment components in Fig. 5 can be expressed as follows:

$$M_x = \bar{M}_{x'} \tag{1}$$

$$M_{z'} = M_x \frac{du}{dz} \tag{2}$$

$$M_{y'} = \bar{M}_{x'} \phi \tag{3}$$

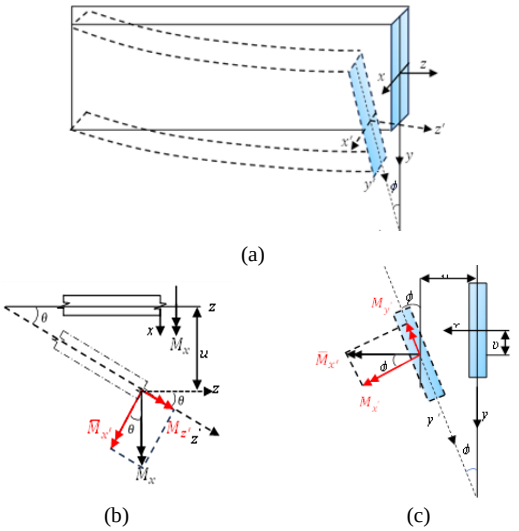

(a) (b) (c)

Fig. 5. Lateral-torsional buckling behaviour of a rectangular glass beam.

Assuming that the magnitude of u, v, and ϕ are very small, the differential equations for the equilibrium in the critical state for the buckled beam are:

$$EI_x \frac{d^2 v}{dz^2} = M_x \tag{4a}$$

$$EI_y \frac{d^2 u}{dz^2} = \phi M_x \tag{4b}$$

$$GJ \frac{d\phi}{dz} = -\left(\frac{du}{dz}\right) M_x \tag{4c}$$

where GJ is the torsional stiffness and EI the bending stiffness. By differentiating Eq. (5c) with respect to z, eliminating $d^2\phi/dz^2$ and combining Eqs. (4c) with 4(b), it is obtained that:

$$GJ \frac{d^2\phi}{dz^2} + \frac{M_x^2}{EI}\phi = 0 \tag{5}$$

Therefore, the Euler's theoretical critical moment is:

$$M_{cr} = \frac{\pi}{l}\sqrt{EI\ GJ} \tag{6}$$

Several studies of literature established efficient analytical models for glass buckling, based on the buckling curve concept [14-17].

Basically, the governing parameters for the LTB verification are usually referred to the typical in-plane bending resistance (M_{res}) and actual load-bearing capacity (M_u) of the beam. The nominal resistance M_{res} depends on the tensile strength of glass (σ_r) and on the elastic section modulus ($W_x = 1/6\, ht^2$ for a rectangular section):

$$M_{res} = \sigma_r W_x \tag{7}$$

The buckling reduction factor for LTB ($\chi_{LT} = M_u/M_{res}$) is then efficiently implemented through LTB buckling curves (i.e., Fig. 6), to verify the actual bending failure moment (M_u) and the effective capacity of the member. Finally, the slenderness ratio is given by:

$$\lambda_{LT} = \sqrt{\sigma_r W_x / M_{cr}} \tag{8}$$

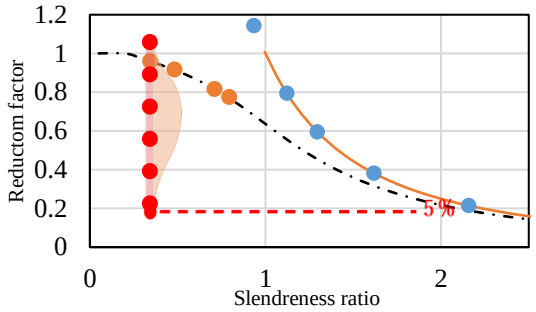

Fig. 6. Design buckling curve based on normal distribution of experimental data (example).

3. EXPERIMENTS

3.1 Setup

Fig. 7 depicts a schematic view of the experimental frame arrangement that was arranged in support of present investigation. Each glass specimen was subjected to two vertical loads (500 mm each from the ends) that were gradually increased in a quasi-static monotonic protocol, until collapse. Ther bending and LTB response parameters were monitored as discussed in [11].

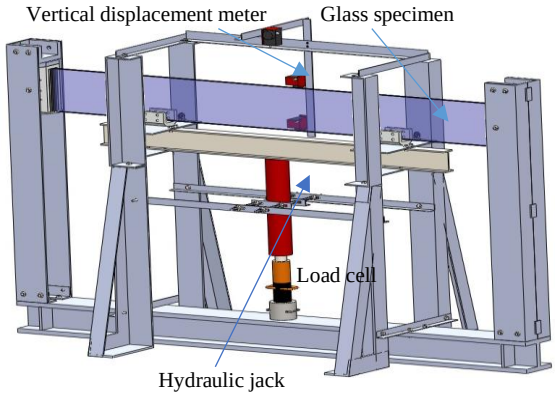

Fig. 7. Experimental setup.

3.2 Specimens

Glass is a linear elastic material until tensile failure, having a Young's modulus of 70 MPa and a Poisson's ratio of 0.23 (ρ= 2500 kg/m^3 its density). The geometrical features of tested specimens (approximately 10 in total in each series) are described in Table 1.

Table 1. Features of tested specimens.

Thickness (t) mm	Length (l) mm	Height (h) mm	No. of tests
8, 10, 12	2000	130, 150, 180, 200	10 each (52 in total)

3.3 Results

The experimental outcomes and evidences were thoroughly assessed to derive useful details in support of the allowable stress calculation. Typical load-displacement records can be seen in Fig. 8(a). Basically, the specimens initially responded elastically with a pure in-plane bending mechanism. Nonetheless, most of them experienced rapid out-of-plane bending and LTB (Fig. 8(b)), which often resulted in very large amplitudes for

the recorded displacement components and even sudden brittle collapse (Fig. 8(c)).

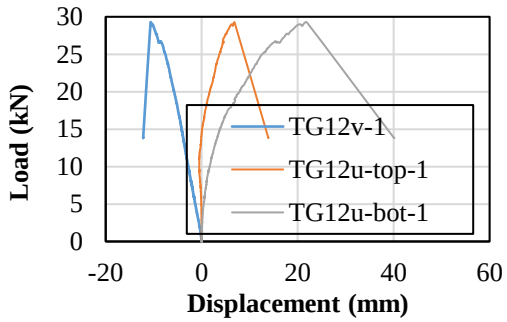

(a) Load-displacement measurements.

(b) Lateral-torsional buckling deformation.

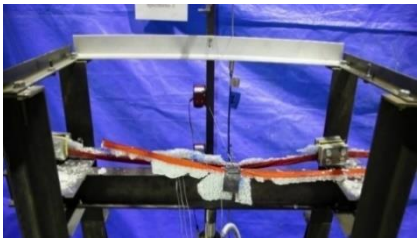

(c) Sudden failure.

Fig. 8. Selection of experimental observations.

4. EXPERIMENTAL EVALUATION OF THE ALLOWABLE BENDING STRESS

4.1 Basic Theory of Allowable Design Concept

The analysis of experimental results proved that medium-large slenderness ratio (i.e., $\lambda_{LT} \geq 1.25$) closely match the theoretical Euler's buckling curve for LTB, while small ratios (i.e., $\lambda_{LT} < 1.25$) diverge from classical theory (see Fig. 9). After analysing the available data distribution, the authors defined the minimum allowable stress to ensure a 95% safety level [7], and address typical structural issues for member safety.

4.2 Statistical Calculation

For the collected experimental results, see Fig. 9, the normal distribution of $x = M_u/M_{cr}$ ratio for a given slenderness was set in the probability range of 5% of the log-normal distribution of data. The lower limit parameter, defined as $C = (x - \mu)/\bar{\sigma}$, was determined considering that:

$$f(x) = \frac{1}{\bar{\sigma}\sqrt{2\pi}} exp\left(-\frac{(x-\mu)^2}{2\bar{\sigma}^2}\right) \quad (9)$$

By imposing that:

$$I(\infty \geq Z \geq C) = \int_0^{\infty} f(z)dz = 95\% \quad (10)$$
$$\Rightarrow C = -1.6449$$

it was finally obtained:

$$\bar{M}_{cr} = (\mu - 1.6449\,\bar{\sigma})M_{cr;avg} \quad (11)$$

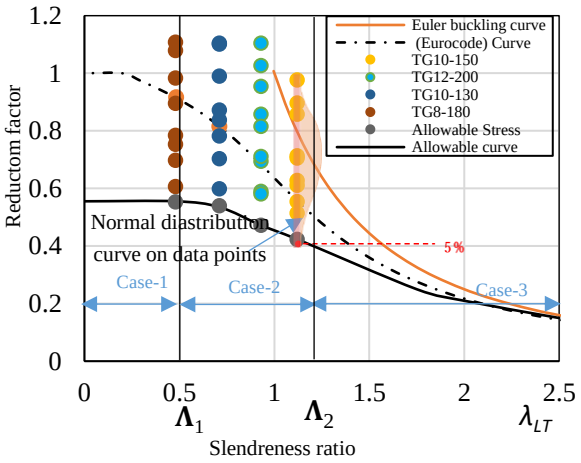

Fig. 9. Statistical analysis of allowable stress and moment.

4.3 Allowable Bending Stress Formulation

Based on experimental evidences and elaborations like in Fig. 9, a formulation was finally developed to facilitate the calculation of the allowable bending stress for glass beams under in-plane loads. For practical efficiency, the methodology detects three cases / ranges of slenderness ratio, which are typically associated to different failure mechanisms.

Case 1: brittle behaviour ($\lambda_{LT} < \Lambda_1 = 0.5$)
When a load-bearing member exhibits brittle collapse, substantial structural deformation cannot take place before failure. An appropriate safety check should account for the material behaviour and member capacity under both long-term (L) and short-term (S) loads. This suggests that the allowable bending stress for design could be expressed as:

$$f_{L,b} = \frac{1}{3}\ \alpha_L\ \gamma\ \bar{\sigma}_c \quad (12a)$$
$$f_{s,b} = \frac{2}{3}\ \alpha_S\ \gamma\ \bar{\sigma}_c \quad (12b)$$

where α_L and α_S are safety factors (to define).
The ratio $\sigma_t = \gamma\ \bar{\sigma}_c \approx 0.57\ \bar{\sigma}_c$ is derived by the authors in previous studies, to express the tensile strength as a function of the compressive one [9].

Case 2: inelastic critical buckling ($\Lambda_1 = 0.5 \leq \lambda_{LT} < \Lambda_2 = 1.25$)
Before LTB, compared to "Case 1", the member experiences considerable elastic deformation. When the material can offer considerable flexibility but the slenderness ratio is still relatively small ($\Lambda_2 < \lambda_{LT}$), this is the typical observed mechanism. The allowable bending stress in this specific scenario can be expressed as the fitting curve of minimum experimental data (i.e., based on Fig. 9), which means:

$$f_b = 0.57\bar{\sigma}_c\ (-0.21\lambda_{LT}^2 + 0.12\lambda_{LT} + 0.54) \quad (13)$$

and for long/short-term loads results respectively in:

$$f_{L,b} = \frac{1}{3}[f_b] \quad (14a)$$
$$f_{S,b} = \frac{2}{3}[f_b] \quad (14b)$$

Case 3: elastic buckling ($\lambda_{LT} \geq \Lambda_2 = 1.25$)
Elastic buckling is the typical outcome of a member that bends elastically and is often characterized by a medium-

large slenderness. The Euler's buckling formula, which has been adjusted for LTB, can potentially be employed to determine the critical stress, and results in:

$$f_{L,b} = \frac{\pi \alpha_L}{3}\left(\frac{C_b}{W_x l_b}\sqrt{EI\ GJ}\right) \quad (15a)$$

$$f_{S,b} = \frac{2\pi \alpha_S}{3}\left(\frac{C_b}{W_x l_b}\sqrt{EI\ GJ}\right) \quad (15b)$$

5. TRIAL STRUCTURAL DESIGN

5.1. Reference Configuration and Approach

To demonstrate that the promoted approach can be efficiently used for real structures, a trial design was finally carried out. The reference model for the trial structural design, see Fig. 9(a), consists in a spatial structure spanning 16×16 m. The Lap-panel framework of Fig. 2 is used for the roof, which is made of tempered glass and cladded by rectangular tempered glass panels (Fig. 9(b)). Spring joints are interposed to provide an appropriate structural interaction (Fig. 9(c)).

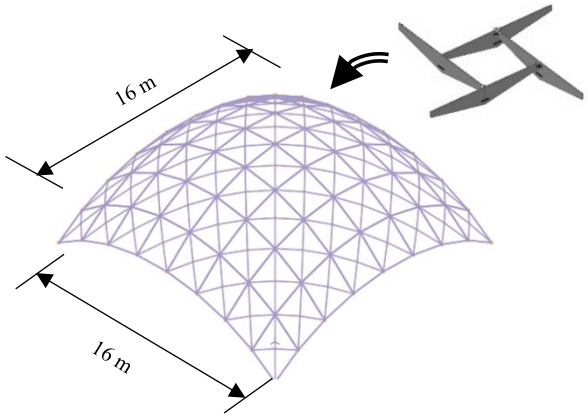

(a) Full-scale model.

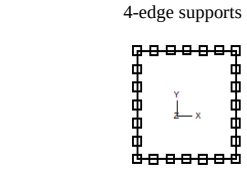

(b) Pin boundary condition.

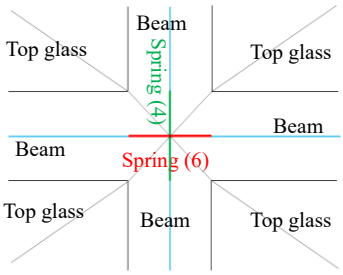

(c) Schematic detail of spring joints.

Fig. 9. Trial structural design.

The herein promoted approach assumes that the supporting glass panels can be transformed into equivalent, beams with identical bending and axial stiffness (Fig. 10(a)), while the roof panels are transformed in crossing beams, that are required to offer an identical shear stiffness to the three-dimensional assembly (see Fig. 10 and [11]).

After analysing the equivalent beams and calculating the maximum stresses due to the assigned design actions (i.e., dead and seismic loads), the allowable stress can be finally checked to satisfy the resistance verification.

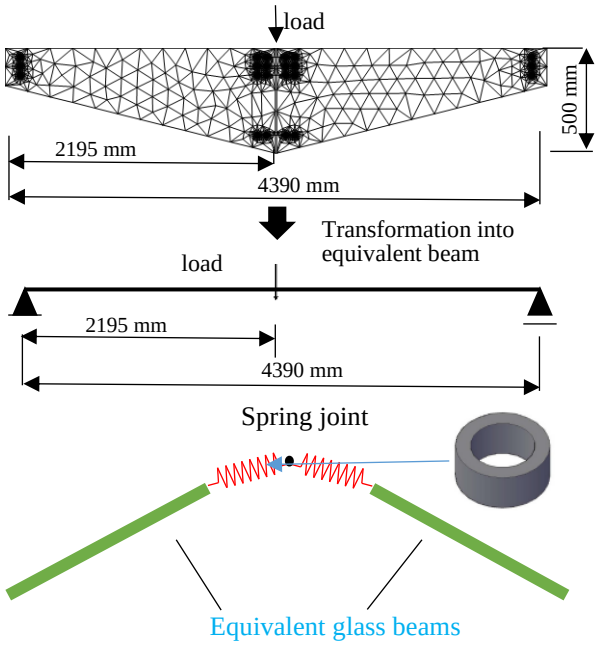

Rubber material is used between the bolt and hole (spring constant) to allow local deformations

(a) Transformation process into equivalent beam

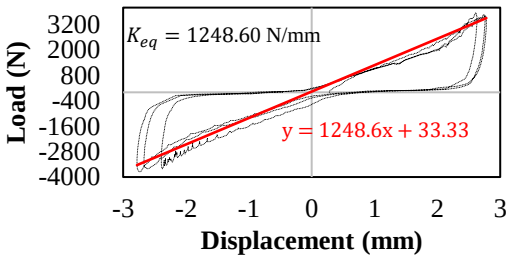

(b) Constitutive law of spring joints [7].

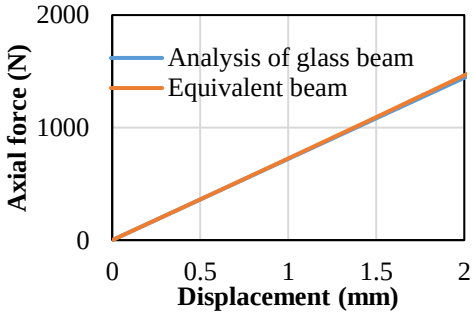

(c) Mechanical analysis of real and equivalent beams.

Fig. 10. Transformation process and mechanical analysis of glass panels as equivalent beams.

5.2. Design Loads and Dynamic Parameters

The dead (long-term) load can be determined by summing the weight of glass and aluminium components, while the design seismic load (short-term) derives from standards.

More precisely, the equivalent static seismic load can be conventionally calculated based on [9], where:

$$Acc(i_q) = \sum_{j=1} \beta_{jq} S_A(T_j, h_j) u_{iqj} \quad (16a)$$

$$Acc'(i_q) = \frac{Acc(i_q)}{max(Acc(i_q))} Acc_{max};\ Acc_{\max} = 0.3 \quad (16b)$$

$$P_{iq} = Acc'(i_q) \times w_{iq} \quad (16c)$$

and $Acc(i_q)$ indicates the distribution of the amplification factor for seismic load at point i of direction q; β_{jq} indicates the participation factor of eigen-mode j; S_A is the spectral acceleration of mode j with period T_j and damping factor h_j; and u_{iqj} denotes the q component of the eigen-vector of mode j at point i. Consequently, $Acc'(i_q)$ indicates the amplification factor for seismic load (with a maximum Acc_{max}= 0.3), which is a common value for the earthquakes of middle and small scales in Japan.

By the eigen-value analysis of the three-dimensional system (with lumped masses due to dead load at each joint), the obtained eigen-modes are shown in Fig. 11, and the corresponding vibration periods / participation factors are summarized in Table 2. Finally, the distribution of the amplification factors is modelled as shown in Fig. 12).

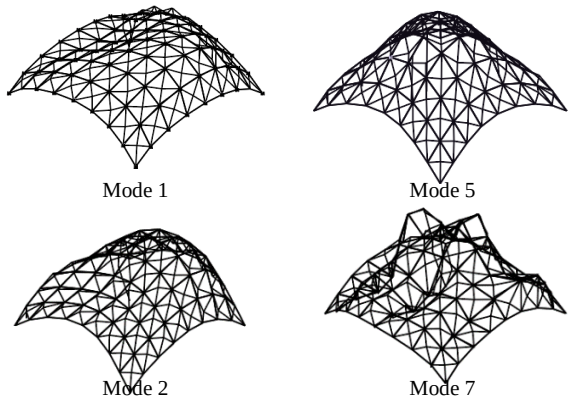

Fig. 11. Eigen-value analysis (selected modes).

Table 2. Vibration periods and participation factors.

Mode	Period (s)	Participation factor		
		X	Y	Z
1	0.1125	-0.022	7.715	0.186
2	0.327	0.735	0.130	-3.920
3	0.321	-3.462	0.032	-0.771
4	0.277	-0.001	-0.027	0.012
5	0.272	0.010	0.231	1.766
6	0.279	1.0458	0.078	-0.115
7	0.273	0.177	-2.310	0.189
8	0.229	-0.050	-0.003	-0.011
9	0.223	-2.806	0.175	-0.072
10	0.217	-0.300	-2.356	0.030

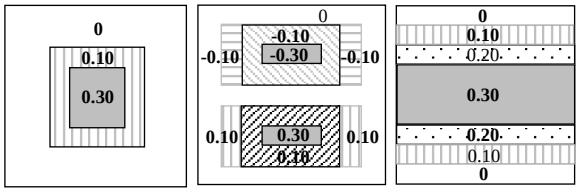

(a) Vertical symmetry (b) Vertical asymmetry (c) Horizontal

Fig. 12. Distribution of amplification factors for seismic load application.

5.3. Stress Verification

Following the approach proposed in Section 4, the reference slenderness ratio for the examined members is estimated in $\lambda_{LT} = 0.91$, which corresponds to "Case 2" of the developed methodology.

The associated allowable bending stress for design is estimated from Eq. (13), and overall results in $f_b = 0.57\bar{\sigma}_c(0.48) = 65.66$ N/mm^2, where $\bar{\sigma}_c = 240$ N/mm^2 is the average compressive strength from previous experimental investigations [9]. From Section 4, the long-term allowable bending stress can be thus estimated as:

$$f_{L,b} = \frac{1}{3}[f_b] = 21.88 \text{ N/mm}^2$$

Table 3 reports the final result of such a stress verification, which was carried out with the support of a Finite Element numerical analysis, to determine the stress peaks in the examined member (see Fig. 13).

Table 3. Allowable bending stress verification under long-term (dead) load.

Stress due to long-term load		Max. stress (N/mm^2)	Allowable (N/mm^2)	Check
X-direction Glass beam	Axial	6.63	21.88	OK
	Bending	8.06	21.88	OK
Y-direction Glass beam	Axial	6.47	21.88	OK
	Bending	7.89	21.88	OK

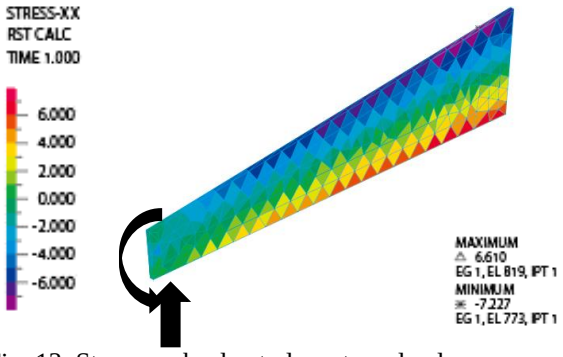

Fig. 13. Stress peaks due to long-term load.

For short-term (seismic) loading, a similar approach can be taken into account, where:

$$f_{S,b} = \frac{2}{3}[f_b] = 43.78 \text{ N/mm}^2$$

Typical results are summarized in Table 4 and Fig. 14.

Table 4. Allowable bending stress verification under short-term (seismic) load.

Stress due to short-term load		Max. stress (N/mm^2)	Allowable (N/mm^2)	Check
X-direction Glass beam	Axial	13.25	43.78	OK
	Bending	15.58	43.78	OK
Y-direction Glass beam	Axial	16.54	43.78	OK
	Bending	14.62	43.78	OK

As a final remark, in terms of deformations of the examined frameless glass system, the maximum displacement under dead load was quantified in ≈47 mm, while for a middle-scale earthquake it raised up to ≈58 mm. Accordingly, additional verification checks should be also carried out at the global and local levels.

Besides, most importantly, the herein reported mechanical analysis confirmed that the maximum stress in glass panels resulting from dead (long-term) and seismic (short-term) loads does not exceed the proposed allowable bending stress, as also verified with the support of a more refined Finite Element numerical study.

Overall, the presented findings prove that the suggested methodology and structural system concept (i.e., the spatial frameless glass structure design with the Allowable Stress Method) can be efficiently developed for future explorations and extensions.

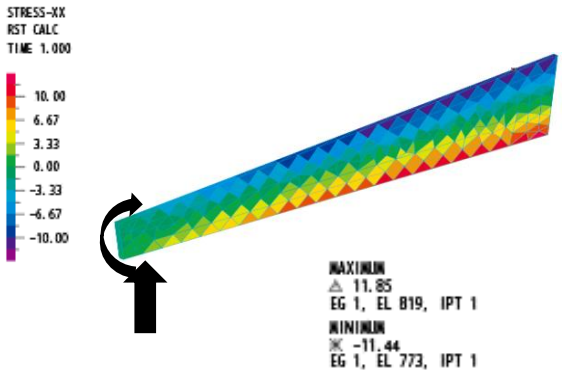

Fig. 14. Stress peaks due to short-term load.

6. Conclusion

In this paper, a generalized methodology was presented to promote the development of three-dimensional frameless glass structures for spatial constructions.

A structural design approach that converts the complex glass panels into equivalent beams (with identical bending and axial stiffness) was presented. This concept was further supported by a sound proposal for the prediction of the allowable bending stress for similar members, based on their slenderness ratio parameter.

A practical design example was also finally discussed, to emphasize the potential of the presented approach and its possible future extension for additional configurations. In this regard, many significant issues should be also further investigated to ensure structural safety, such as more sophisticated seismic considerations in dynamic regime, fatigue phenomena, durability or even fireproofing. In any case, the present study poses the basis and tracks new research efforts in this direction.

Acknowledgements

Research staff from the University of Trieste, Department of Engineering and Architecture (Italy), and Kyushu Institute of Technology (Japan) are gratefully acknowledged for having facilitated the scientific collaboration between the involved authors.

Data availability

Datasets generated or analysed in the current study will be shared upon reasonable request.

7. REFERENCES

[1] Murtyas, S., Ridwan, M., & Budiarto, R. (2019). Occupancy Rate and Water Utility Effects on Energy Consumption of Commercial Building: Case Study Grand Inna Malioboro Hotel in Indonesia. In Proceeding of International Exchange and Innovation Conference on Engineering & Sciences (IEICES). Interdisciplinary Graduate School of Engineering Sciences, Kyushu University.

[2] Website: https://www.ionglass.co.uk/product/how-to-fix-structural-glass-beams-to-glass-fins

[3] Bedon, C., Amadio, C., Noé, S.: Safety issues in the seismic design of secondary frameless glass structures. Safety 5(4), 80 (2019).

[4] Chen, P. S., & Tsai, M. T. (2019). On configuration and structural design of frameless glass structures. In Structures and Architecture-Bridging the Gap and Crossing Borders (pp. 628-637). CRC Press.

[5] Chen, P. S., & Tsai, M. T. (2019). On configuration and structural design of frameless glass structures. In Structures and Architecture-Bridging the Gap and Crossing Borders (pp. 628-637). CRC Press.

[6] S. Hussain, P.S. Chen, N. Koizumi, B. Liu, X. Yan, Experimental study on spring constants of structural glass panel joints under in-plane loading, Pertanika Journal of Science & Technology 31 (4) (2023).

[7] Hussain, S., Chen, P.S., Matsuno, Y., Liu, B.: Experimental report on compression loading test of tempered glass panels. In: Awam International Conference on Civil Engineering AICCE 2022) (LNCE, volume 385), USM, Malaysia (2022)

[8] Hussain, S., Bedon, C., Kumar, G., Ahmed, Z.: Bayesian regularization backpropagation neural network for glass beams in lateral-torsional buckling. Adv. Civil Eng. (2023).

[9] Chen, P.S., Hussain, S., Matsuno, Y.: Experimental report on glass panels against static and repeated in-plane compression loading. J. Struct. Eng. B 69, 225–231 (2023).

[10] Hussain, S., Chen, P.S., Koizumi, N., et al.: Feasibility of computational intelligent techniques for the estimation of spring constant at joint of structural glass plates: a dome-shaped glass panel structure. Glass Struct. Eng. 8, 141–157 (2023)

[11] Hussain, S., Chen, P. S., Hassanlou, D., Bolhassani, M., & Bedon, C. (2024). Bending and lateral-torsional buckling investigation on glass beams for frameless domes. Results in Engineering, 21, 101962.

[12] Saddam et al 2024: In-Plane Bending Behavior of Single-Layer Glass Beams in Frameless Glass Structure Proceedings of 6th International Conference on Civil Engineering and Architecture, Vol. 1 ICCEA 2023, LNCE 530, pp. 1–11, 2024.

[13] Rumbayan, R., & Rumbayan, M. (2019). A Study on The Utilization of Local Coconut Timber Waste as Sustainable Building Material. In Proceeding of International Exchange and Innovation Conference on Engineering & Sciences (IEICES) (Vol. 5, pp. 1-3). Interdisciplinary Graduate School of Engineering Sciences, Kyushu University.

[14] Amadio, C., & Bedon, C. (2010). Buckling of laminated glass elements in out-of-plane bending. Eng Struct, 32: 3780-3788.

[15] Belis, J., Bedon, C., Louter, C., Amadio, C., & Van Impe, R. (2013). Experimental and analytical assessment of lateral torsional buckling of laminated glass beams. Eng Struct, 51: 295-305.

[16] Amadio, C., & Bedon, C. (2013). A buckling verification approach for monolithic and laminated glass elements under combined in-plane compression and bending. Eng Struct, 52: 220-229.

[17] Bedon, C., & Amadio, C. (2015). Design buckling curves for glass columns and beams. ICE Proceedings Struct. Build., 168(7) :514-526.